Vol 16 No 6, June 2007
1009-1963/2007/16(06)/1736-07

Chinese Physics

© 2007 Chin. Phys. Soc.
and IOP Publishing Ltd

Effect of lithium-potassium mixed alkali on spectroscopic properties of Er^{3+}-doped aluminophosphate glasses*

Fang Yong-Zheng(房永征)[a)b)†], Liao Mei-Song(廖梅松)[a)], and Hu Li-Li(胡丽丽)[a)]

[a)] *Shanghai Institute of Optics and Fine Mechanics, Chinese Academy of Sciences, Graduate School of the Chinese Academy of Sciences, Shanghai* 201800, *China*
[b)] *Shanghai Institute of Technology, Shanghai* 200023, *China*

(Received 20 October 2006; revised manuscript received 29 December 2006)

Er^{3+}-doped lithium-potassium mixed alkali aluminophosphate glasses belonging to the oxide system $x$$K_2O$-(15-$x$)$Li_2O-4B_2O_3-11Al_2O_3$-5BaO-65$P_2O_5$ are obtained in a semi-continuous melting quenching process. Spectroscopic properties of Er^{3+}-doped glass matrix have been analysed by fitting the experimental data with the standard Judd–Ofelt theory. It is observed that Judd–Ofelt intensity parameters $\Omega_t (t = 2, 4 \text{ and } 6)$ of Er^{3+} change when the second alkali is introduced into glass matrix. The variation of line strength $S_{ed}[^4I_{13/2}, ^4I_{15/2}]$ follows the same trend as that of the Ω_6 parameter. The effect of mixed alkali on the spectroscopic properties of the aluminophosphate glasses, such as absorption cross-section, stimulated emission cross-section, spontaneous emission probability, branching ratio and the radiative lifetime, has also been investigated in this paper.

Keywords: non-crystalline materials, mixed alkali, radiative lifetime, Judd–Ofelt theory
PACC: 7000, 7855, 7840, 3350D

1. Introduction

Er^{3+}-doped glasses have received much attention due to their capability of producing the emission in the communication window of 1.54 μm.[1−10] The laser at this wavelength is located in an 'eyesafe' spectral region and could be detected easily.[11,12] Phosphate glass is considered to be the best matrix for erbium glass laser because of high gain coefficient, wide bandwidth capability, low upconversion emission, high solubility of rare earth ions and low probability of energy back transfer from Er^{3+} to Yb^{3+}. In addition, phosphate glasses can be produced at a relatively low temperature and easily processed.[13]

The mixed alkali effect (MAE) is one of the problems in glass science and has been studied for some decades. The MAE corresponds to a deviation from linearity of some physical properties, which is caused by substituting one alkali by a second one. Mixed alkali glass is considered as an important kind of material in the sense of science and technology. Different models have been proposed to explore the origin of this phenomenon in the literature and are summarized in several review papers.[14−16] In spite of extensive investigations, there appears to exist no universally accepted mechanism responsible for the various mixed alkali effects.

The mixed alkali effect has not been studied much in aluminophosphate glasses. Also, reports on spectroscopic studies are very few but they are important and useful for acquiring some insight into the microscopic mechanism responsible for the effect. Our previous work has presented the effect of mixed alkali on phase transformation kinetics of aluminophosphate glasses.[17] In this respect, the aim of the present work is to characterize the effect of mixed alkali on the spectroscopic properties of Er^{3+}-doped aluminophosphate glasses.

2. Experiments

The glass samples with the composition of $x$$K_2O$–(15-$x$)$Li_2O$–4$B_2O_3$–11$Al_2O_3$ –5BaO–65P_2O_5 (where x = 0, 3.75, 7.5, 11.25 and 15 mol%) were externally doped each with 1mol% Er^{3+}, which were in-

*Project supported by the Young Teacher Foundation of Shanghai Education Committee (Grant No 04YQHB162) and the National Natural Science Foundation of China (Grant No 50572110).
†Corresponding author. E-mail: fangyzh@yahoo.com.cn

troduced as Er_2O_3. Reagent grade commercial oxides (> 99.9% pure) were used as the starting materials for glasses preparation. In order to remove bubbles and striae and to obtain homogeneous optical glass, a semi-continuous melting process was adopted. Glasses were first melted in a fused quartz crucible and then transferred to a platinum crucible at 1300 °C. To reduce OH^- content in glasses, all melts were bubbled with oxygen flowing through heated CCl_4 liquid. After refining, melts were cast into a steel mould, annealed to room temperature with a cooling rate of 5 °C/min, then cut and polished into 2 mm × 10 mm × 20 mm size for spectroscopic measurements. The density of the glass was measured with the Archimedes method. The absorption spectra were measured using a Perkin-Elmer UV/VIS/NIR LAMDA 9 spectrophotometer. The fluorescence spectra were measured with a Triax 550 Spectrofluorimeter under 980 nm LD excitation. Fluorescence lifetime of $^4I_{13/2}$ level of Er^{3+} was detected by a HP546800B100-MHz oscilloscope. Refractive indices were obtained through the V-prism method. All the measurements were carried out at room temperature.

3. Results and discussion

3.1. Absorption spectrum and Judd–Ofelt intensity parameters

The absorption spectra of Er^{3+}-doped glasses with different K_2O contents are shown in Fig.1. The inhomogeneously broadened bands are assigned to the transitions from the $^4I_{15/2}$ ground state to the excited states of Er^{3+} ions, and each excited level of Er^{3+} is marked. The broadening of the absorption bands results from the absence of long-range order in the host producing changes in the microsymmetry around the Er^{3+} ion. The transition $^4I_{15/2}$-$^4I_{13/2}$ is important for amplifiers operating in the 1.5 μm communication window. For the Judd–Ofelt analysis, seven absorption bands corresponding to the absorptions from the ground state $^4I_{15/2}$ to the excited states $^4I_{11/2}$, $^4I_{9/2}$, $^4F_{9/2}$, $^4H_{11/2}$, $^4F_{7/2}$, $^2H_{9/2}$, $^4G_{11/2}$, respectively are taken into account and the peak energies in cm^{-1} for different transitions have been used in the calculations. Some transitions ($^4I_{13/2}$, $^4S_{3/2}$, $^4F_{5/2}$) are excluded for contributions to magnetic dipole transition, weak intensity or overlapping of their absorption bands. The calculated electric-dipole line strength S_{ed} for electric-dipole transition between an initial state $|aJ\rangle$ and a final state $|bJ'\rangle$ is given by

$$S_{ed} = \sum_{t=2,4,6} \Omega_t |\langle aJ||U^{(t)}||bJ'\rangle|^2 = \Omega_2 \times u_2^2 + \Omega_4 \times u_4^2 + \Omega_6 \times u_6^2, \quad (1)$$

where $\left|\langle aJ\left|\left|U^{(t)}\right|\right|bJ'\rangle\right|$ is the reduced matrix element of unit tensor operator for the corresponding transition, which can be expressed in u_2^2, u_4^2 and u_6^2 with corresponding values of Ω_t and considered to be not strongly host-dependent.[18] $\Omega_t (t = 2, 4, 6)$ is the Judd–Ofelt parameter.

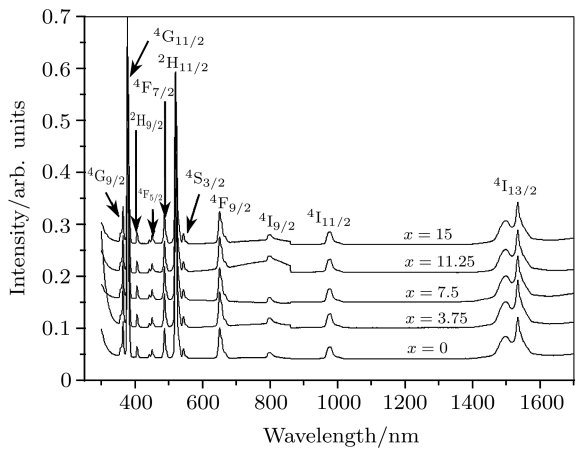


Fig.1. Optical absorption spectra of Er^{3+} doped xK_2O-(15-x)Li_2O-4B_2O_3-11Al_2O_3-5BaO-65P_2O_5 glasses.

For the transitions between states which follow the rules $\Delta S = \Delta L = 0, \Delta J = 0, \pm 1$ there exists the contribution of magnetic dipole transition, which is expressed as

$$S_{md} = \frac{1}{4m_e^2c^2}\left|\langle (S,L)J||L+2S||(S',L')J'\rangle\right|^2, \quad (2)$$

where c represents the velocity of light, and m_e is the mass of the electron.

Furthermore, the experimental S_{ed} can be calculated with the experimental values of the integrated absorbance by

$$\int \kappa(\lambda)\mathrm{d}\lambda = \frac{8\pi^3e^2\lambda_m N}{3hc(2J+1)}\frac{(n^2+2)^2}{9n}S[aJ;bJ'], \quad (3)$$

where $\int \kappa(\lambda)\mathrm{d}\lambda$ is the integrated absorption coefficient and can be calculated from the absorption spectrum of each absorption band, λ_m is the mean wavelength of the absorption peak, h is Planck's constant, c is the velocity of light, e is the electron charge, J is the quantum number of angular momentum of the initial state, n is the refractive index, N is the concentration of rare-earth ions in a unit volume. The Judd–Ofelt parameters Ω_t for Er^{3+}-doped lithium-potassium mixed

alkali aluminophosphate glasses are obtained by fitting the electrical dipole contributions to the experimental line strengths of the observed transitions to the calculated ones by using the least square method. $S_{\rm ed}$ is dependent on glass structure and composition, but $S_{\rm md}$ is independent of ligand fields.

The Judd–Ofelt theory[19,20] is a most useful theory in estimating the probability of the forced electric dipole transitions of rare-earth ions in various environments. The Judd–Ofelt intensity parameters Ω_t (t = 2, 4, 6) contain the effects of the crystal field terms, radial integrals of an electron, and so on.

Figure 2 shows the Ω_t parameters of mixed alkali glass samples as a function of K_2O concentration. Taking into account all the errors occurring in the integrated absorption cross section obtained with Perkin-Elmer, calculated concentration and measured thickness, the error of Ω_t is estimated to be ±5%. According to the previous studies,[21,22] the large value of Ω_2 reflects the asymmetry and high covalency of Er^{3+} and ligands.[23] The stronger the interaction between Er^{3+} and oxygen ions, the larger the value of Ω_2. As Jorgensen and Reisfeld [21] reported, the Ω_4 and Ω_6 parameters are associated with the rigidity of the medium in which the ions are situated; parameter Ω_6 decreases with increasing covalency of chemical bond between rare earth and ligand atoms which can be adjusted by the composition of glass host. The high values of Ω_6 represent the enhancement in ionicity between rare earth and ligand atoms and induce a large Stark splitting in the energy levels of Er^{3+} ions, which results in a large inhomogeneous broadening and wide emission band.[24,25] It is observed from Fig.2 that Ω_4 and Ω_6 increase when a second alkali is added to glass matrix. At 7.5mol% K_2O, the parameters Ω_4 and Ω_6 reach their corresponding maxima. It is indicated that there exists a low covalency between erbium cation and oxide anion and thus a high covalency of lithium-potassium mixed alkali aluminophosphate glass hosts. In addition, high values of Ω_4 and Ω_6 show high rigidity in mixed alkali glasses. Different from Ω_4 and Ω_6, the parameter Ω_2 has two high value peaks at 3.75mol% K_2O and 11.25mol% K_2O respectively and a low peak at 7.5mol% K_2O. This can be explained by effects of mixed alkali on the asymmetry and high covalency of Er^{3+} and ligands. On the one hand, the covalency of Er^{3+} and ligands decreases and thus Ω_2 reduces due to the effect of mixed alkali in glasses, and on the other hand, the effect of mixed alkali can also lead to the increase of the asymmetry in glass host. A large number of different sites in glasses and lower symmetry, in which the rare-earth ions are situated, contribute to a high value of Ω_2. At 3.75mol% K_2O and 11.25mol% K_2O, the effect of mixed alkali on the asymmetry in glass host is predominant, which leads to two peaks (high Ω_2). A lower Ω_2 is gained at 7.5mol% K_2O because the effect of mixed alkali on covalency of Er^{3+} and ligands is predominant. Furthermore, it can be seen from Fig.2 that the $S_{\rm ed}[^4I_{13/2}, {}^4I_{15/2}]$ parameter follows the same trend as that of the Ω_6 parameter. According to the Judd–Ofelt theory, the line strength of $S_{\rm ed}$ of the 1.55 μm corresponding to $^4I_{13/2} \rightarrow {}^4I_{15/2}$ transition can be obtained as follows:[26]

$$S_{\rm ed}[^4I_{13/2}, {}^4I_{15/2}] = 0.0188\Omega_2 + 0.1176\Omega_4 + 1.4617\Omega_6. \quad (4)$$

This formula shows that $S_{\rm ed}$ is mainly determined by Ω_6 because of its relatively large coefficient of 1.4617, thus, $S_{\rm ed}$ is also considered as a reflection of broadband evaluation.

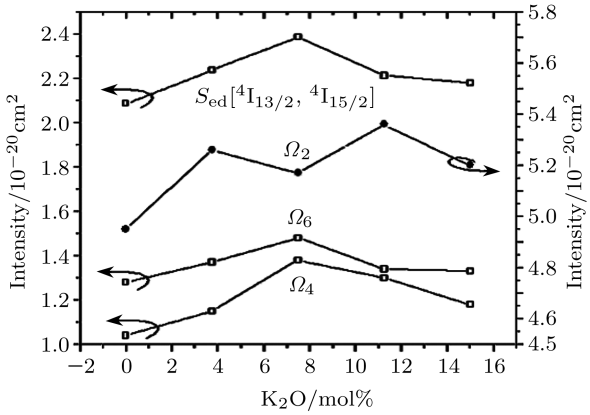


Fig.2. Judd–Ofelt parameters Ω_t (t = 2, 4, 6) and the line strength of $S_{\rm ed}$ corresponding to $^4I_{13/2} \rightarrow {}^4I_{15/2}$ transition as a function of K_2O concentration in glasses. Lines are drawn as guides for the eye.

3.2. Absorption cross-section and stimulated emission cross-section

The absorption cross-section of Er^{3+}, $\sigma_{\rm abs}(\lambda)$ is calculated according to the expression[27]

$$\sigma_{\rm abs}(\lambda) = \frac{2.303\log(I_0/I)}{Nl}, \quad (5)$$

where I_0/I is optic density ratio which can be gained from the absorption spectrum, N is the ion concentration of Er^{3+}, l is the sample thickness. The stimulated

emission cross-section of Er^{3+}, $\sigma_{emi}(\lambda)$ can be calculated according to the McCumber theory[28] from the absorption cross-section $\sigma_{abs}(\lambda)$ as follows:

$$\sigma_{emi}(\lambda) = \sigma_{abs}(\lambda) \exp\left(\frac{\varepsilon - hc\lambda^{-1}}{\kappa T}\right), \quad (6)$$

where h, c, k, λ, and T represent the Planck's constant, velocity of light, Boltzmann constant, room temperature, wavelength, respectively. ε can be calculated from the following expression:

$$\frac{N_1}{N_2} = \exp(\varepsilon/kT), \quad (7)$$

where N_1 and N_2 are the equilibrium populations of $^4I_{15/2}$ and $^4I_{13/2}$ levels at a temperature of T without optical pumping, respectively. According to the approximate calculation,[29] we have

$$\exp(\varepsilon/kT) \approx 1.1 \exp(E_0/kT), \quad (8)$$

where E_0 is the energy interval between the lowest manifolds of $^4I_{13/2}$ and $^4I_{15/2}$ levels.

Figure 3 illustrates the calculated absorption cross-sections (σ_{abs}) and stimulated emission cross-sections (σ_{emi}) of Er^{3+} ions as a function of wavelength in glass $7.5K_2O$-$7.5Li_2O$-$4B_2O_3$-$11Al_2O_3$-$5BaO$-$65P_2O_5$. As σ_{abs} and σ_{emi} diagrams of other glasses are similar in shape, they have not been shown in the figure. It is found that the peaks of absorption cross-section and stimulated emission cross-section of erbium are around 1533 nm (λ_p). At a wavelength longer than λ_p, σ_{emi} is larger than σ_{abs}, otherwise, σ_{emi} is smaller than σ_{abs}. The peak absorption and emission cross-sections are 5.91×10^{-21} cm^2 and 6.05×10^{-21} cm^2 at 1.533 μm respectively.

Figure 4 shows the peak absorption and emission cross-sections of Er^{3+} at 1.533 μm varying with K_2O concentration in $x$$K_2O$–(15-$x$)$Li_2O$–$4B_2O_3$–$11Al_2O_3$–$5BaO$–$65P_2O_5$ glasses. It is observed that the peak absorption and emission cross-sections of Er^{3+} increase largely when a second alkali is added to glass matrix (K_2O = 3.75mol%) because the coexistence of Li_2O and K_2O induces the mixed alkali effect. However, with the further increase of K_2O content, the peak absorption and peak emission cross-sections show little variations. For single alkali glasses (K_2O=0 or 10mol%), the peak absorption and the peak emission cross-sections are similar.

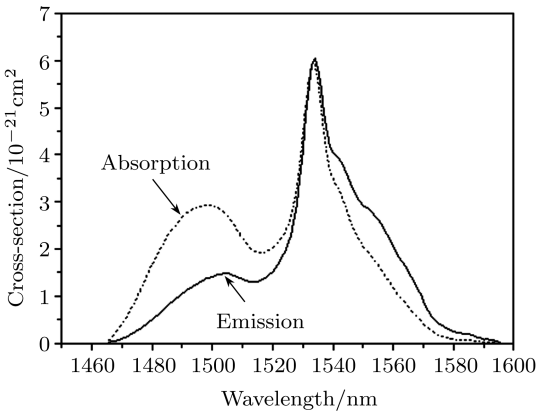


Fig.3. Absorption cross-section and the stimulated emission cross-section calculated by McCumber theory of Er^{3+} in glass $7.5K_2O$–$7.5Li_2O$–$4B_2O_3$– $11Al_2O_3$–$5BaO$–$65P_2O_5$.

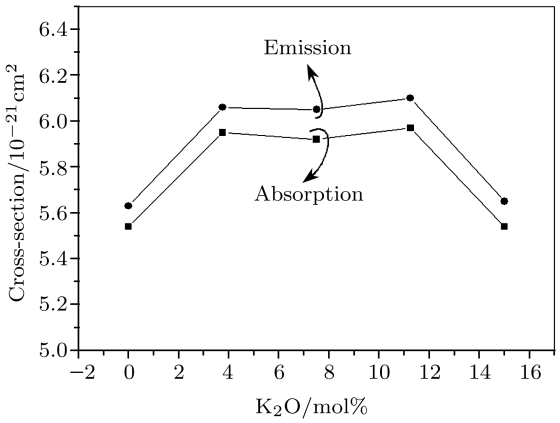


Fig.4. The peak absorption and the peak emission cross-sections of Er^{3+} vs K_2O concentration in $x$$K_2O$–(15-$x$)$Li_2O$–$4B_2O_3$– $11Al_2O_3$–$5BaO$–$65P_2O_5$ glasses at 1.533 μm.

3.3. Spontaneous emission probability, branching ratio and the radiative lifetime

The spontaneous emission probability A_{rad} (aJ, bJ') is given by

$$A_{rad}(aJ, bJ') = A_{ed} + A_{md} = \frac{64\pi^4 v^3 e^2}{3h(2J+1)} \left[\frac{n(n^2+2)^2}{9} S_{ed} + n^3 S_{md}\right], \quad (9)$$

where A_{ed} and A_{md} are the electric-dipole and magnetic-dipole spontaneous emission probabilities, respectively.

Table 1. Predicted spontaneous emission probabilities A_{rad}, branching ratios β, and radiative lifetimes τ_{rad} for Er^{3+} in $x$$K_2O$–(15-$x$) Li_2O–4B_2O_3–11Al_2O_3–5BaO–65P_2O_5 glasses.

		$x = 0$			$x = 3.75$			$x = 7.5$			$x = 11.25$			$x = 15$		
Transitions	Average frequency /cm^{-1}	$A_{JJ'}$ /s^{-1}	β	τ_{rad} /ms	$A_{JJ'}$ /s^{-1}	β	τ_{rad} /ms	$A_{JJ'}$ /s^{-1}	β	τ_{rad} /ms	$A_{JJ'}$ /s^{-1}	β	τ_{rad} /ms	$A_{JJ'}$ /s^{-1}	β	τ_{rad} /ms
$^4I_{13/2} \rightarrow {}^4I_{15/2}$	6535	117.5	1	8.51	124.9	1	8.0	127.5	1	7.8	120.9	1	8.27	121.3	1	8.24
$^4I_{11/2} \rightarrow {}^4I_{15/2}$	10244	110	0.86	7.79	119	0.86	7.2	125	0.86	6.9	114	0.86	7.5	115	0.86	7.4
$^4I_{13/2}$	3079	18.4	0.14		19.4	0.14		20.09	0.14		18.9	0.14		18.9	0.14	
$^4I_{9/2} \rightarrow {}^4I_{15/2}$	12563	70	0.54	7.6	78.1	0.55	7.03	73.5	0.52	7.1	85.6	0.58	6.8	79.1	0.56	7.1
$^4I_{13/2}$	6028	36.9	0.28		39.9	0.28		42.8	0.31		38.1	0.26		38.3	0.27	
$^4I_{11/2}$	2319	23.9	0.18		24.2	0.17		23.99	0.17		23.56	0.16		23.88	0.17	
$^4F_{9/2} \rightarrow {}^4I_{15/2}$	15314	980	0.90	0.92	1080	0.90	0.83	1080	0.88	0.81	1110	0.90	0.81	1070	0.90	0.84
$^4I_{13/2}$	8779	48.9	0.04		53.7	0.04		53	0.04		55.6	0.04		53.2	0.04	
$^4I_{11/2}$	5070	58.9	0.05		63.6	0.05		91.5	0.07		61.2	0.05		61.4	0.05	
$^4I_{9/2}$	2751	2.83	0.01		3.05	0.01		2.98	0.01		3.03	0.01		2.98	0.01	
$^4S_{3/2} \rightarrow {}^4I_{15/2}$	18349	1060	0.67	0.60	1140	0.67	0.59	1230	0.67	0.55	1090	0.67	0.61	1100	0.67	0.61
$^4I_{13/2}$	11814	433	0.27		469	0.28		503	0.27		447	0.27		450	0.27	
$^4I_{11/2}$	8105	34.4	0.02		37.3	0.02		39.8	0.02		35.8	0.02		35.9	0.02	
$^4I_{9/2}$	5786	53.6	0.04		58.3	0.03		61.0	0.04		57.3	0.04		56.6	0.03	

The radiative lifetime $\tau_{\rm rad}$ of an emitting state aJ is calculated from

$$\tau_{\rm rad} = \frac{1}{\sum\limits_{bJ'} A_{\rm rad}(aJ, bJ')^{-1}}. \qquad (10)$$

The fluorescence branching ratio of transitions from initial manifold aJ to lower levels bJ' is given by

$$\beta(aJ, bJ') = \frac{A_{\rm rad}(aJ, bJ')}{\sum\limits_{bJ'} A_{\rm rad}(aJ, bJ')^{-1}}. \qquad (11)$$

The calculated spontaneous emission probability $A_{\rm rad}$, branching ratio β and the radiative lifetime $\tau_{\rm rad}$ are listed in Table1. Figure 5 shows the variations of radiative lifetime $\tau_{\rm rad}$ for $^4I_{13/2}$ and $^4I_{11/2}$ levels with K_2O concentration in glasses. The lifetime of $^4I_{13/2}$ level of Er^{3+} is also an important parameter for optical amplifier or laser applications in the 1.54 μm band. The longer lifetime of $^4I_{13/2}$ level benefits the population inversion between the $^4I_{13/2}$ and $^4I_{15/2}$ levels. In addition, the longer lifetime of $^4I_{11/2}$ of Er^{3+} will lead to a strong reverse energy transfer in Er–Yb codoped glass, enhancing the up-conversion losses. Thus, the relatively long lifetime of $^4I_{11/2}$ of Er^{3+} in Er–Yb codoped glass will not allow efficient lasing at 1.54 μm. Comparing with single alkali glasses (K_2O = 15mol% or 0mol%), the mixed alkali glasses have a short lifetime of $^4I_{13/2}$ and achieve a shortest lifetime at 7.5mol% K_2O (see Fig.5). The lifetime of $^4I_{11/2}$ level of Er^{3+} shows a similar trend to that of $^4I_{13/2}$ and obtains its minimum also at 7.5mol% K_2O. However there is no appreciable change in the branching ratios (see Table1). The variation of the radiative lifetime $\tau_{\rm rad}$ with K_2O increasing can be explained by refractive index of glass hosts. According to Eqs.(9) and (10), the radiative lifetime $\tau_{\rm rad}$ calculated by the Judd–Ofelt theory is inversely proportional to refractive index of the glass hosts. It can be seen from Fig.5 that the radiative lifetime shows an inverse trends with K_2O increasing.

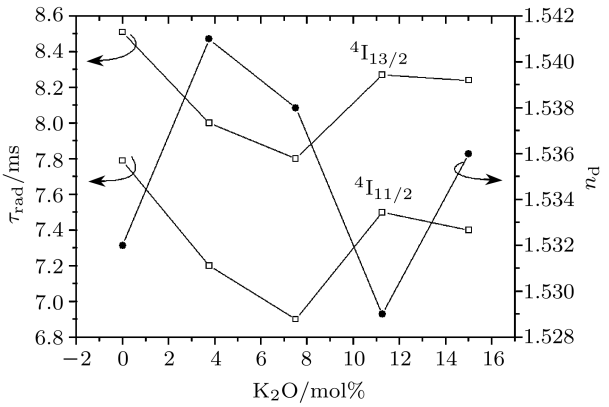


Fig.5. Calculated radiative lifetime for Er^{3+} emitting states of $^4I_{13/2}$ and $^4I_{11/2}$ versus K_2O concentration in glasses. Lines are drawn as guides for the eye.

4. Conclusions

Based on the Judd–Ofelt theory and absorption spectrum, the optical parameters have been calculated, such as Judd–Ofelt parameters Ω_t (t = 2, 4, 6) and the line strength of electric-dipole transition. The effect of mixed alkali on the asymmetry and covalency of chemical bond between rare earth and ligand atoms has been discussed according to the variations of the Judd–Ofelt intensity parameters. It is found that the parameters Ω_4 and Ω_6 can reach their corresponding maxima at 7.5mol% K_2O while Ω_2 shows two peaks with the variations of K_2O and Li_2O contents in glass matrix. The line strength of electric-dipole transition $S_{\rm ed}[^4I_{13/2}, {}^4I_{15/2}]$ follows the same trend as that of the parameter Ω_6. By using the McCumber theory, we have obtained the absorption cross-section and emission cross-section of Er^{3+} in glasses matrix. The spontaneous emission probability, the branching ratio and the fluorescence lifetime of each excited level are also calculated and discussed.

References

[1] Mao Y L, Sun Z R, Jiang X L, Deng P Z and Gan F X 2002 *Chin. Phys.* **6** 613
[2] Zhao C, Zhang Q Y and Jiang Z H 2006 *Chin. Phys.* **15** 2158
[3] Duan S Q, Tan N and Zhang Q Y 2005 *Chin. Phys.* **3** 615
[4] Su F N and Deng Z D 2006 *Chin. Phys.* **15** 1096
[5] Xu SQ, Fang D W, Zhang Z X, Zhao S L, Zhang L Y, Wang B L and Jiang Z H 2005 *Chin. Phys.* **14** 2246
[6] Li T, Zhang Q Y, Zhao C, Feng Z M, Shi D M, Deng Z D and Jiang Z H 2006 *Chin. Phys.* **14** 1250
[7] Liu Z P, Hu L L, Zhang D B, Dai S X, Qi C H and Jiang Z H 2002 *Acta Phys. Sin.* **51** 2629 (in Chinese)
[8] Dai S X, Yang J H, Liu Z P, Wen L, Hu L L and Jiang Z H 2003 *Acta Phys. Sin.* **52** 729 (in Chinese)
[9] Xu S Q, Wang G N, Zhang J J, Dai S X, Hu L L and Jiang Z H 2004 *Acta Phys. Sin.* **53** 1840 (in Chinese)
[10] Yang Z M, Zhang Q Y, Liu Y H and Jian Z H 2005 *Acta Phys. Sin.* **54** 2013 (in Chinese)

[11] Edwards J Q and Sandoe J N 1974 *J. Phys.* D **7** 1078
[12] Snitzer E, Woodcock R and Sergre J 1968 *IEEE J. Quantum Electron.* **QE-4** 360
[13] Sales B S and Boatner L A 1984 *Science* **226** 45
[14] Isard J O 1969 *J. Non-Cryst. Solids* **1** 235
[15] Day D E 1976 *J. Non-Cryst. Solids* **21** 343
[16] Ingram M D 1987 *Phys. Chem. Glasses* **28** 215
[17] Fang Y Z, Liao M S and Hu L L 2006 *Thermochimica* **443** 184
[18] Carnall W T, Fields P R and Wybourne B G 1965 *J. Chem. Phys.* **42** 3797
[19] Judd B R 1962 *Phys. Rev.* **127** 750
[20] Ofelt G S 1962 *J. Chem. Phys.* **37** 511
[21] Jorgensen C K and Reisfeld R 1983 *J. Less-Common Method* **93** 107
[22] Balda R, Fernandez J and Sanz M 2000 *Phys. Rev.* B **62** 3384
[23] Heidepriem H E, Ehrt D, Bettinelli M and Speghini A 1998 *J. Non-Cryst. Solids* **240** 66
[24] Tanabe S 1999 *J. Cryst. Solids* **259** 1
[25] Tanabe S 1993 *J. Appl. Phys.* **73** 8451
[26] Webber M J 1964 *Phys. Rev.* **157** 262
[27] Miniscalco W J and Quimby R S 1991 *Opt. Lett.* **16** 258
[28] McCumber D E 1964 *Phys. Rev.* A **134** 299
[29] Miniscalco W J and Quimby R S 1991 *Opt. Lett.* **16** 258